Bulletin of the Seismological Society of America, Vol. 100, No. 5A, pp. 1971–1988, October 2010, doi: 10.1785/0120090189

Earthquake Fault Scaling: Self-Consistent Relating of Rupture Length, Width, Average Displacement, and Moment Release

by Mark Leonard

Abstract In this paper, I propose the scaling relation $W = C_1 L^{\beta}$ (where $\beta \approx 2/3$) to describe the scaling of rupture width with rupture length. I also propose a new displacement relation $\bar{D} = C_2\sqrt{A}$, where A is the area (LW). By substituting these equations into the definition of seismic moment ($M_0 = \mu \bar{D} LW$), I have developed a series of self-consistent equations that describe the scaling between seismic moment, rupture area, length, width, and average displacement. In addition to β, the equations have only two variables, C_1 and C_2, which have been estimated empirically for different tectonic settings. The relations predict linear log–log relationships, the slope of which depends only on β.

These new scaling relations, unlike previous relations, are self-consistent, in that they enable moment, rupture length, width, area, and displacement to be estimated from each other and with these estimates all being consistent with the definition of seismic moment. I interpret C_1 as depending on the size at which a rupture transitions from having a constant aspect ratio to following a power law and C_2 as depending on the displacement per unit area of fault rupture and so static stress drop. It is likely that these variables differ between tectonic environments; this might explain much of the scatter in the empirical data.

I suggest that these relations apply to all faults. For small earthquakes ($M < \sim 5$) $\beta = 1$, in which case L^3 fault scaling applies. For larger ($M > \sim 5$) earthquakes $\beta = 2/3$, so $L^{2.5}$ applies. For dip-slip earthquakes this scaling applies up to the largest events. For very large ($M > \sim 7.2$) strike-slip earthquakes, which are fault width-limited, $\beta = 0$ and assuming $\bar{D} \propto \sqrt{A}$, then $L^{1.5}$ scaling applies. In all cases, $M_0 \propto A^{1.5}$ fault scaling applies.

Introduction

The theoretical and empirical versions of fault rupture area to seismic moment relations give very similar results. However, this is not the case for rupture length to seismic moment relations, where the relations differ significantly. This inconsistency between empirical and theoretical results raises the question of whether the empirical results are as robust as their statistical uncertainties would indicate. A related problem is that published empirical relations are not self-consistent. By self-consistent, I mean relations that enable seismic moment, fault length, width, area, and displacement to be estimated from each other, with all these relations being consistent with the definition of seismic moment. That is, if you start with one parameter (e.g., fault length) and determine all of the others (area, width, displacement, moment), you retrieve the same set of parameters, no matter which parameter you start with.

Resolving these issues has important consequences for several areas of seismology. For example, palaeoseismology is an important field of seismology that has the potential to significantly improve our understanding of long-term earthquake hazard. Palaeoseismology is based on the ability to estimate the magnitude and number of causative earthquake(s) from the measured scarp length and displacement. Consequently, robust scaling relations are key to this process, because the accuracy of the inferred earthquake magnitude and occurrence rates are dependent upon the quality of the assumed relationship between rupture dimension and magnitude. Real-time tsunami scenario modelling, for warning purposes, requires robust estimates of rupture length and displacement based solely on moment. Also, modern probabilistic earthquake and tsunami risk modelling involves simulating thousands of earthquakes and estimating the effect of each earthquake. Each simulated earthquake requires fault dimensions, displacement, magnitude, hypocenter, and orientation. Accurate results require that the rupture dimension, displacement, and moment to be consistent. The Wells and Coppersmith (1994) relations (WC94) are commonly used in such applications.

The purely empirical WC94 relations are not self-consistent and so their applicability to such simulation processes is not ideal. Because many of the WC94 results for reverse (thrust) faults are not statistically significant, their applicability is unclear. For intraplate continental regions the dataset they compiled did not include sufficient earthquakes to produce any relations. Although many other scaling relations have been published, they tend to be developed for a narrow class (e.g., large strike-slip) of earthquakes and often only for a subset of measures (e.g., $M_0 \sim L$).

Theoretical and empirical scaling relations between magnitude and area ($M \sim A$) are similar. Using the definitions of M_0 and M_w, it can be shown that an earthquake with a stress drop of 3 MPa has a theoretical scaling relation $M = 1 \log A + 4$ (see Table 1 for a list of abbreviations used in this paper, and see Hanks and Bakun (2002) for details of the derivation). Several authors have developed empirical relations (e.g., $M = 0.98 \log A + 4.07$ from WC94), which, within the statistical uncertainties, are identical to the theoretical relation. This observation has been used by some authors to fix the slope and so calculate self-similar scaling relations (e.g., Somerville *et al.*, 1999, where $M = \log A + 3.95$; Hanks and Bakun, 2002, where $M = \log A + 3.98$).

Table 1
Variables and Abbreviations in This Paper

	Explanation
Variable	
L	Fault rupture length (km). This is the subsurface horizontal fault rupture length; where only surface rupture length is available this has been used.
SRL	Surface rupture length (km)
RLD	Subsurface horizontal rupture length (km)
W	Fault width; the down-dip fault rupture width (km)
r	Radius of a circular fault
A	Fault area ($L * W$ for a rectangular fault) (km^2)
$\bar{D}$	Average fault displacement (m)
D_{av}	Average surface displacement (m)
D_{max}	Maximum surface displacement (m)
μ	Shear modulus (MPa or Nm^{-2})
M_0	Scalar moment ($M_0 = \mu \bar{D} A$) (Nm)
M_w	Moment magnitude ($M_w = 2/3 \log M_0 - 6.07$)
M	Magnitude, normally M_w or equivalent
$\Delta\sigma$	Stress drop (MPa or Nm^{-2})
C	Constant
β	Power exponent used in scaling relations
C_1	Constant used in scaling relations ($m^{1-\beta}$)
C_2	Constant used in scaling relations
δ	Constant used relating $\log M_0$ to $\log L$
γ	Constant used relating $\log M_0$ to $\log A$
Abbreviation	
SCR	Stable Continental Regions. Intraplate continental crust that has not been extended by continental rifting. It is a subset of Scholz (2002) type III regions.
C	Constant
WC94	Wells and Coppersmith (1994)

In contrast to relationships between magnitude and area, theoretical and empirical scaling relations between magnitude and rupture length are not similar. By assuming that faults scale with a constant aspect ratio, displacement scales with fault width in a linear fashion and following the approach of Hanks and Bakun (2002), mentioned previously, simple dislocation theory leads to the theoretical relation $M = 2 \log L + 3.9$. This is very different from the corresponding WC94 relation of $M = 1.5 \log L + 4.4$. That the empirical slope is 1.5 implies that $M_0 \propto L^{2.25}$ is inconsistent with the general assumption that $M_0 \propto L^3$. Note that the previous discussion does not apply to large width-limited strike-slip earthquakes. The consistency between theoretical and empirical M–A scaling relations is in marked contrast to the inconsistency between the M–L scaling relations. This paper addresses this inconsistency.

For large fault width-limited strike-slip earthquakes, where the fault aspect ratio is greater than 4, there have been extensive discussions in the literature on the implications of displacement to length scaling models on length to moment scaling. Whether displacement scales linearly with fault width or length or some intermediate relation remains an open question. In this debate, there has been little discussion of the inconsistency between theoretical and empirical length to seismic moment relations, or of the area to length scaling implied by these relations. With most authors focusing on a single dataset (e.g., $M_0 \sim A$ or $M_0 \sim L$) and ignoring the others, it has been difficult to compare their results.

This paper is divided into two parts. In part, I propose a new rupture area scaling relation, which, by relating width to length via a power law, accounts for the change in aspect ratio with increasing M_0. I then use this relation to develop a series of $\log M_0 \sim \log A$ and $\log M_0 \sim \log L$ relations that depend only on the choice of displacement model, and then use the $W \sim L$, $M_0 \sim A$, and $M_0 \sim L$ data to determine a preferred displacement model. In Part 2: Empirical Scaling Relations, I empirically estimate the scaling constants for a variety of earthquakes types. The resultant scaling relations, unlike most previous relations, are self-consistent.

Previous Work

The observation that seismic moment scales with fault area to the power 3/2 is one of the longest standing relations in modern seismology. The linearity between $\log M_0$ and $\log A$ is well documented (Aki, 1972; Thatcher and Hanks, 1973; Kanamori and Anderson, 1975; Abe, 1975; Geller, 1976; Hanks, 1977; Kanamori, 1977). This linearity is interpreted to be due to constant average stress drop (Chinnery, 1969) and is consistent with theoretical moment and stress drops for simple rupture geometries (e.g., circular faults, Brune, 1970, 1971), which assume L^3 scaling. Aki (1972) concluded that shallow focus earthquakes have a constant stress drop of 1–10 MPa. This has been refined over the

years, with interplate and intraplate earthquakes considered to have typical stress drops of 2.5–3.5 MPa and 5–10 MPa, respectively. It is worth noting that the method used to calculate stress drops affects the value. Traditionally, stress drop was calculated using the equation for stress drop (equation 1) (Aki, 1972; Kanamori and Anderson 1975), with the Brune stress model becoming more common in the digital age (Atkinson and Beresnev, 1997). Models other than the simple Brune stress model, such as those of Haskell (1966), Sato (1972), and Madariaga (1978), will generally give different results, as will fault rupture inversions, such as those of Somerville *et al.*, 1999.

Once a fault's width approaches the width of the seismogenic zone, strike-slip earthquakes become fixed width and the fault expands only in length. There has been extensive discussion in the literature for this class of faults on whether the seismic moment scales with width (W or L^1 scaling) or length (L^2 scaling) (Scholz, 1982; Romanowicz, 1992; Romanowicz and Rundle, 1993; Romanowicz, 1994; Scholz, 1994a; Bodin and Brune, 1996; Pegler and Das, 1996; Scholz, 1997, 1998; Hanks and Bakun, 2002). While most authors now agree that L^1 scaling applies (Shaw and Scholz, 2001; Romanowicz and Ruff, 2002; Manighetti *et al.*, 2007), much of the debate may have occurred because the limited data available were dominated by what Scholz (2002) called the crossover regime earthquakes, where faults have an aspect ratio between 2 and 10. Once more data for large earthquakes with a high aspect ratio (>4) were available, a preference for L^1 scaling became clearer. Romanowicz and Ruff (2002) demonstrated that much of the scatter in the scaling data could be explained by L^3 and L^1 scaling, but with different tectonic environments having slightly different constants due to differing fault strengths. Using a different dataset, Hanks and Bakun (2002, 2008) proposed an L^2 scaling model. In this debate there was little discussion of the process of transitioning from fixed aspect faults (which is required of L^3 scaling) to faults with an aspect ratio of >4.

Recent work suggests that in the crossover regime (i.e., L approximately 20 to 100 km) neither model alone applies, with several authors (Bodin and Brune, 1996; Mai and Beroza, 2000) concluding that slip is between the W and L scaling models. The dataset used by Mai and Beroza (2000) was derived from fault rupture modelling rather than aftershock mapping, so their results, to some extent, provide an independent test of most other empirical work, which generally uses aftershock mapping (e.g., Wells and Coppersmith (1994); Pegler and Das, 1996; Shaw and Scholz, 2001; Romanowicz and Ruff, 2002; Hanks and Bakun, 2002). Using numerical modelling, both Bodin and Brune (1996) and Shaw and Scholz (2001) proposed a two-regime $D-L$ model that preserved constant stress drop. Manighetti *et al.* (2007), building on this work, suggested that the variability in data could be explained by the different crustal properties in various tectonic environments. King and Wesnousky (2007) proposed a simple asymmetric wedge slip function, which for large earthquakes extends below the seismogenic zone. This slip distribution both maintains constant stress drop and is observed to slowly increase average displacement with length. Shaw and Wesnousky (2008) suggested that by allowing significant coseismic slip below the seismogenic layer, constant stress drop is maintained over the entire spectrum of earthquake sizes. Using these ideas, Shaw (2009) developed fault-scaling relations for large strike-slip faults, which in the crossover regime has intermediate slip and follows the W model for very large ($L > 100$ km) earthquakes. Like Hanks and Bakun (2002, 2008), they explicitly assume that faults scale with a constant aspect ratio, of ~1, until they reach the width of the seismogenic zone (~15 km), and then become fixed width.

There has been comparatively little discussion in the literature of fault-scaling relations for dip-slip faults. Henry and Das (2001), using a dataset of interplate dip-slip earthquakes, which expanded on the Wells and Coppersmith (1994) data, found that the aspect ratio of the earthquake rupture increases with length and that slip is proportional to length for moment $M_0 < 3 \times 10^{21}$ Nm. Within uncertainties, their relations are the same as WC94. Stirling *et al.* (2002) combined several databases of instrumental and preinstrumental earthquakes for both strike-slip and dip-slip mechanisms, in order to investigate discrepancies between magnitude estimates from intensity and scaling relations. They suggest that large ($M_w > 6.5$) earthquakes scale differently to small earthquakes and proposed new relations, which differ from WC94, for estimating moment and displacement from surface rupture length.

In midcontinental crust or stable continental regions (SCR), the available data are small. Wells and Coppersmith (1994) state: Because the SCR datasets for surface rupture length and displacement relationships contain only six or seven earthquakes and the correlations are low ($r < 0.75$), these relationships are not significant at a 95% probability and are not considered further. In SCR some investigators (e.g., Somerville *et al.*, 1999, 2001) use relations akin to $M = \log A + 4$, but add 0.3–0.4 to account for an assumed higher stress drop. The most widely accepted relation for scaling magnitude and length for SCR earthquakes is that of Johnston (1994) ($M = 1.36 \log \mathrm{SRL} + 4.67$). However, because it is based on only 10 to 12 earthquakes, it is purely empirical and is not well constrained.

Data

Several published datasets have been used in this paper. The data have been divided into two categories: plate boundary, which includes interplate and plate boundary related (Scholz *et al.*, 1986, Class I and Class II) earthquakes, and stable continental region (SCR), which includes midcontinental (Scholz *et al.*, 1986, Class III) earthquakes. The data are predominately plate boundary earthquakes.

The datasets include Wells and Coppersmith (1994), Henry and Das (2001), Hanks and Bakun (2002),

Romanowicz and Ruff (2002), and Manighetti *et al.* (2007). The Henry and Das (2001) data significantly expand the number of large thrust earthquakes included compared with the WC94 data. Romanowicz and Ruff (2002) and Manighetti *et al.* (2007) also expand the number for strike-slip earthquakes compared with the WC94 data. The Manighetti *et al.* (2007) data are very similar to the data of Shaw and Scholz (2001). For the 2004 Sumatra–Andaman earthquake, two dimensions are considered here: a length of 1400 km and width of 150 km, and a length of 800 km and width of 140 km. The first dimension is consistent with aftershock mapping (Engdahl *et al.*, 2007; Vallie, 2007), tsunami modelling (Fuji and Satake, 2007), and geodetic and seismic slip modelling (Rhie *et al.*, 2007). It is used in the statistical analysis. The second dimension accounts for 85% of coseismic moment release (Chlieh *et al.*, 2007) and, while plotted, is not included in the statistical analysis.

The bulk of the rupture dimensions in these datasets were estimated from aftershock mapping, with the displacements and surface rupture lengths being from scarp data. The Somerville *et al.* (1999) data used rupture modelling to estimate the rupture dimensions, as did a component of the Manighetti *et al.* (2007) data. As the number of earthquakes with dimensions derived from rupture models is relatively small and only applies to large strike-slip faults, it is not going to significantly effect the least-squares results. Only data considered by the cited authors to be of good quality have been used in this paper. These data were divided into strike-slip and dip-slip mechanism datasets. Earthquakes of a mixed mechanism were allocated according to the dominant mechanism assigned by the authors of the catalog. Wells and Coppersmith (1994) found that, due to insufficient numbers, many of their thrust fault relations were not statistically significant. To avoid this, and as the WC94 data indicate that there is no statistically significant difference between the scaling properties of reverse and normal faults, I follow the approach of Henry and Das (2001) who combined the reverse and normal data. The data of Henry and Das (2001) contained seven earthquakes that are associated with a larger earthquake that occurred in the preceding weeks or months, and has a longer length, but similar width. These are considered to be associated events, and the smallest of each pair is not included in this analysis.

Johnston (1994) compiled an SCR database of 870 earthquakes where moment could be estimated from either waveform or isoseismal data. This is the source of the SCR data used in this paper. The three Tennant Creek earthquakes (M_w 6.6, 6.3, and 6.2) of 22 January 1988 are a very important contribution to this database, comprising 3 of the 12 surface rupturing earthquakes and three of the five earthquakes with data for all four of SRL, RLD (subsurface horizontal rupture length), D_{av}, and D_{max}. When calculating a relation for $M \sim$ SRL, Johnston (1994) treated the Tennant Creek earthquakes as a single event (M_w 6.76); however, I treat them as three separate events.

Moment and Fault-Scaling Theory

Aki (1966) defined seismic moment as $M_0 = \mu \bar{D} L W$. Kanamori and Anderson (1975) assumed a constant aspect ratio (W/L) when they developed the relations: $M_0 \propto L^3$, $M_0 \propto A^{3/2}$, and $\log M_0 \propto 3/2 M_S$. These relations were used by Kanamori (1977) and Hanks and Kanamori (1979) when they developed the moment magnitude scale (M_w). As noted by Kanamori and Anderson (1975), if the aspect ratio is not constant, then $M_0 \propto A^{3/2}(W/L)^{1/2}$. This can be readily shown by substituting $L_C = W$ into the equation for static stress drop, which is:

$$\Delta\sigma = C\mu\left(\frac{\bar{D}}{Lc}\right) = \frac{CM_0}{ALc}, \tag{1}$$

where L_C is the characteristic rupture dimension that is normally considered the smallest spatial dimension. For a circular fault, L_C is the radius of the fault (Brune, 1970), and for strike-slip faults, $L_C = W$ (Hanks, 1977) is widely accepted. Aki (1972) suggested $L_C = \sqrt{A}$ and incorporated the remainder ($\sqrt{(L/W)}$) into C. Analytical expressions for C and so M_0 have been derived for few special cases, including (from Kanamori and Anderson, 1975):

Circular faults

$$M_0 = 16/7\Delta\sigma r^3, \tag{2}$$

Rectangular dip-slip faults of infinite length

$$M_0 \approx \frac{\pi(\lambda + 2\mu)}{4(\lambda + \mu)}\Delta\sigma W^2 L, \tag{3}$$

Rectangular strike-slip faults of infinite length

$$M_0 \approx \pi\Delta\sigma W^2 L. \tag{4}$$

Both the M_0 relations for rectangular faults assume that $\bar{D} \propto W$. The circular Brune model is routinely used to estimate both M_0 and r from the seismic spectrum and so estimate the stress drop based on the previous formula (e.g., Boore, 1983; Somerville *et al.*, 1987; Atkinson and Boore; 2006). Sato (1972) developed analytical expressions for C for rectangular faults, where $\bar{D} \propto W$ and with aspect ratios $(L/W) < 10$. They showed these faults have a lower stress drop than circular, square, and infinite length rectangular faults of the same width. Relative to a square fault, rectangular dip-slip faults with aspect ratios of 2 and 5 have stress drops 0.86 and 0.71 for dip-slip and 0.7 and 0.51 for strike-slip faults, respectively. For aspect ratios between 1.5 and 6, this can be roughly approximated as $\Delta\sigma \propto (L/W)^{-1/6}$ and $\Delta\sigma \propto (L/W)^{-1/3}$ for dip-slip and strike-slip faults, respectively.

Part 1: Rupture Area Scaling

The width versus length ($W \sim L$) data for normal and reverse dip-slip interplate earthquakes have a linear trend

on a log–log plot (Fig. 1). This increase in aspect ratio with increasing size has been noted previously, with Henry and Das (2001) noting that earthquakes with lengths between 200 and 300 km have aspect ratios of ~3 and between 500 and 900 km have aspect ratios of ~4. They argued that this change in aspect ratio means that W must be taken into account in any discussion of the scaling of L with M_0. Equation (5) is proposed to explain this relationship, where β and C_1 are variables that I empirically fit to the data. From Figure 1 it can be seen that $0 < \beta < 1.0$ for faults of length greater than 5 km.

$$W = C_1 L^{\beta}. \tag{5}$$

Substituting $W = C_1 L^{\beta}$ into $M_0 = \mu \bar{D} L W$ gives $M_0 = \mu \bar{D} L^{1+\beta} C_1$. If average displacement is related to length, width, or area, an equation for earthquake moment that depends only on L, A, or W can be derived. Here I substitute four displacement models into this equation:

1. $\bar{D} = C_2 W$, for which if $\beta \neq 1$ neither $\log M_0 \propto 3 \log L$ nor $\log M_0 \propto 3/2 \log A$ holds.
2. $\bar{D} = C_2 \sqrt{A}$, for which the relation $\log M_0 \propto 3/2 \log A$ holds, but not $M_0 \propto 3 \log L$ if $\beta \neq 1$.
3. $\bar{D} = C_2 L$, for which if $\beta \neq 1$ neither relation holds.
4. $\bar{D} = C_2 L^{2-\beta}$, for which $M_0 \propto 3 \log L$ holds, but not $M_0 \propto 3/2 \log A$ if $\beta \neq 1$.

A generic equation relating moment to area can be written as $\log M_0 = \gamma \log A + \log(C_2 \mu)$ and moment to length as $\log M_0 = \delta \log L + \log(C_1 C_2 \mu)$, where the constant C_2 depends only on the displacement model and the slopes δ and γ depend on both the displacement model and β. The first step is to use the $W \sim L$ data to estimate β, then using this value calculate the expected values of δ and γ. The $M_0 \sim L$ and $M_0 \sim A$ data are then used to determine a preferred displacement model.

In a combination of literature review and their own testing, Wells and Coppersmith (1994) concluded that ordinary least-squares regression of the log of the parameters (e.g., length, width, moment) was the preferred method for analysis of earthquake fault parameters. In this work I follow their approach and use ordinary least-squares regression of the log of the parameters for the regressions.

Determining the Slope (β) in Equation (5)

Analysis of the interplate dip-slip data (Fig. 1), using least squares, gives a slope (β) of 0.668 with a correlation coefficient (r) of 0.94. Excluding the three smallest and four

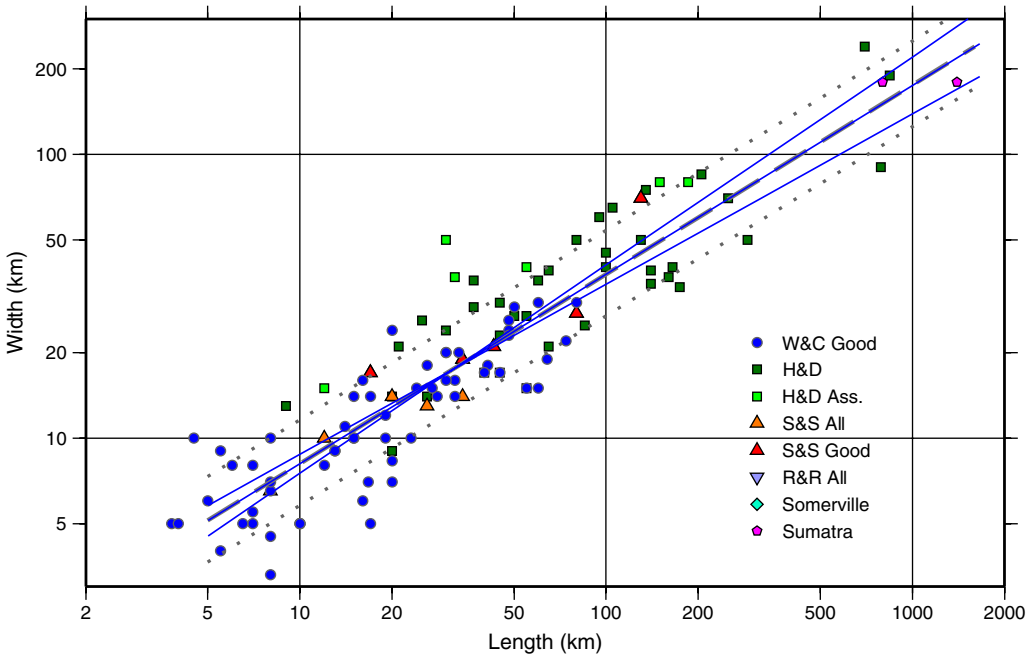

Figure 1. Width versus length for normal and reverse dip-slip interplate faults. The least-squares estimate has a slope of 0.668. The three solid thin lines have slopes of 0.57, 0.67 and 0.73 with a common value at the point of smallest least-squares error. They encompass the range of slopes allowed within the $\pm 1\sigma$ confidence interval. The gray dashed line is defined by $W = C_1 L\beta$, where $\beta = 2/3$ with $C_1 = 1.7$; it has a slope of 2/3 for $5.5 < L < 1500$ km. The gray dotted lines show the 67% confidence interval. The catalogs referred to are W&C for Wells and Coppersmith (1994), H&D for Henry and Das (2001), S&S for the Shaw and Scholz (2001) catalog published in Manighetti *et al.* (2007), R&R for Romanowicz and Ruff (2002), and Somerville is Somerville *et al.* (1999). See text for details on the two values shown for the 2004 M 9.3 Sumatra–Andaman earthquake. This color coding is used in all figures. The color version of this figure is available only in the electronic edition.

largest earthquakes makes little difference, with a slope of 0.658 and r of 0.89. Within the 67% prediction interval (the dashed lines in Fig. 1) slopes of between 0.59 and 0.73 are possible. Given the high variance of the data assuming a value of $2/3$ for β is a reasonable choice. Note that the uncertainties shown in the figures are the prediction interval, not the smaller confidence interval. If faults scaled with a constant aspect ratio, a trend with a slope of 1 would be expected, but this is not the case. The least-squares value of C_1 in equation (5) is 17.5. This power law relation applies up to the largest known megathrust earthquakes with lengths of 1400 km, which corresponds to a width of 220 km.

The Akaike information criteria (Akaike, 1974) is a measure of the goodness of fit of the data to a statistical model, and the model with the smallest AIC is considered the best-fit model. The AIC is commonly used for ranking statistical models (e.g., Shaw, 2009). Here three models are compared: (1) equation (5) with $\beta = 2/3$; (2) a constant aspect ratio of 1.8 ($\beta = 1$, $C_2 = 0.55$), which has the lowest AIC; and (3) an aspect ratio of 1 ($\beta = 1$, $C_2 = 1$). The normalized AIC results for these three models are -144, -71, and 44, respectively. This indicates that the proposed power law model is a significantly better model than any constant aspect ratio model. Setting $\beta = 2/3$ makes the values of δ and γ simple fractions rather than irrational numbers, which would result from using a number such a 0.668.

Note that all seven earthquakes in the Henry and Das (2001) data that were identified previously as having an associated earthquake lie on or above the upper dashed line in Figure 1. If each pair was treated as a single event, the composite event would move to the right and closer to the regression line of Figure 1. Whether there is something unusual about these earthquakes or earthquakes in these regions or simple aleatory uncertainty is not known. Only four earthquakes have a width more than 50% wider than the regression line (Solomon Islands 1979, Hokkaido 1982, Taiwan 1986, and Colombia 1991). For the three earthquakes where width uncertainties are given, the regression line lies within the range of uncertainty.

The interplate strike-slip data are more difficult to analyze. As outlined in the previous discussion on L^1 versus L^2 scaling, it has long been recognized that strike-slip earthquakes become width-limited at widths of 12–20 km. This corresponds to a fault length of 35–60 km; any further increase in rupture area is therefore only as a result of an increase in rupture length. This limits the range of rupture lengths to approximately 4 to 50 km (0.6–1.7 on a log scale), which is much narrower than the dip-slip range of approximately 4–1400 km (0.6–3.1 on a log scale). This makes statistical analysis of strike-slip earthquakes more problematic. At lengths of between 4 and 50 km, it is evident that faults have neither a constant aspect ratio nor a constant width (Fig. 2). The best fit using a constant aspect ratio is 1.25, but it is a poor fit to the data; it underestimates the width of earthquakes with a length less then 10 km and overestimates the width for lengths greater than 20 km. The normalized AIC results for the three models, equation (5) with $\beta = 2/3$, the best fit constant aspect ratio (1.25) model, and an aspect ratio of 1, are -70, -59, and -42, respectively. This indicates that the proposed power law model is a better model than any constant aspect ratio model. Given this result, and in the absence of data suggesting β should be different from the better constrained value for dip-slip earthquakes, $\beta \approx 2/3$ is my preferred value for strike-slip earthquakes. The least-squares value of C_1 in equation (6) is 15.0, so the power relation $W = C_1 L^{\beta}$, $\beta \approx 2/3$, and $C_1 = 15$ is assumed to apply to strike-slip faults between lengths of 4 and 50 km.

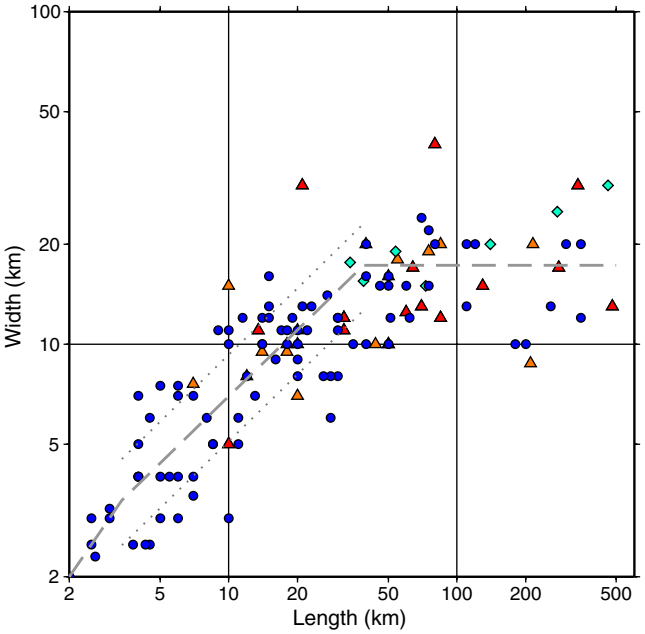

Figure 2. The length versus width data for strike-slip interplate earthquakes. As these faults become width-limited there is a narrow (5–50 km) range of the data that allows a large number of equally valid relations to fit the data. In the 5–50 km range a slope of $2/3$ is assumed from the findings of the dip-slip data. The three gray dashed lines are from 0.5 km to 4 km with a slope of 1, from 4 km to 45 km length with a slope of $2/3$, and a constant width of 17 km at lengths above 45 km. The catalogs are described in Figure 1. The gray dotted lines are the $\pm 1\sigma$ uncertainties. The color version of this figure is available only in the electronic edition.

The SCR (Fig. 3) data contain only eight events. For these data the normalized AIC analysis for fitting equation (5) with $\beta = 2/3$, the best-fit constant aspect ratio (1.4) model, and an aspect ratio of 1 are -4.7, -2.0, and 1.9, respectively. Again the power law relation is the best-fitting model, and the least-squared value of C_1 is 13.5. This analysis suggests that dip-slip earthquakes, whether intraplate or interplate, scale with $\beta = 2/3$.

Determining a Displacement Model

I have demonstrated that the width to length scaling described by equation (5) with $\beta = 2/3$ is a preferred fit

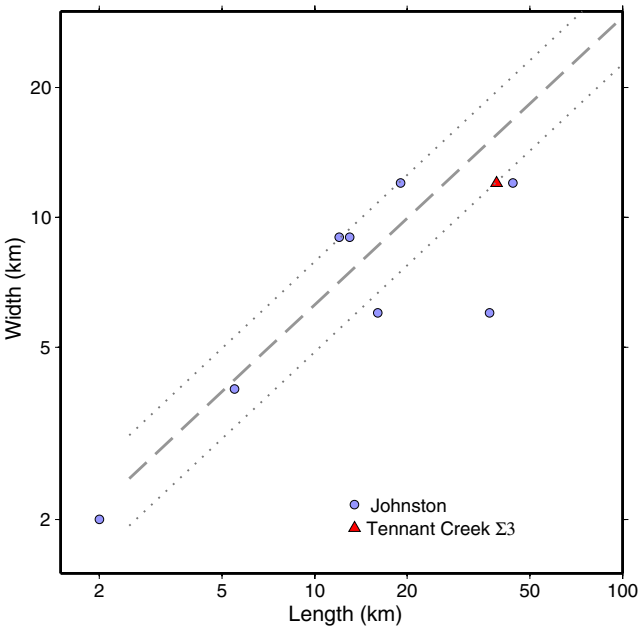

Figure 3. The length versus width data for dip-slip stable continental regions (SCR) earthquake faults. A slope of 2/3 (i.e., $W = C_1 L\beta$, where $\beta = 2/3$) is a good fit to the data. The color version of this figure is available only in the electronic edition.

to the data than any fixed aspect ratio model. This applies to all non-width-limited earthquakes with a length of 5 km or greater. I now use this result to determine a preferred displacement model. Table 2 gives the M_0 equations for the four displacement models and the predicted values for δ and γ for $\beta = 2/3$. Each of these models predicts a different value for the slope, so by comparing these with the empirical data, I test the validity of each displacement model. Note that δ and γ are relatively insensitive to β within the range of 0.6 to 7.3. The $L \sim D$ and $W \sim D$ data have a great deal of scatter, reflecting the high uncertainty in estimating displacement. These data are of little value in differentiating between the four models. The $M_0 \sim L$ and $M_0 \sim A$ data are more promising.

The dip-slip fault $M_0 \sim A$ data (Fig. 4) have a least-squares slope of 0.66 ($\gamma = 1.52$) and r of 0.95, which is very close to the expected value for model II of $\gamma = 1.5$. The dip-slip fault $M_0 \sim L$ data (Fig. 5) have a least-squares slope of 0.37 ($\delta = 2.697$) and an r of 0.92, which is very close to the expected value for model III of $\delta = 2.67$. The higher correlation coefficient of the $M_0 \sim A$ data give a slight preference for model II. From the $M_0 \sim L$ data, the AIC results for the four displacement models are 39, 40, 44, and 58, respectively. For the $M_0 \sim A$ data, the AIC results are 22, 23, 27, and 31, respectively. Model IV consistently ranks last in the AIC rankings, and neither of the least-squared (LS) analyses are consistent with it being the preferred model; as such, I rule it out. The LS analyses give a slight preference to model II over model III, with model I not being preferred for either dataset. The AIC analysis gives a very slight preference to model I over model II, with model III being consistently poorer. The combination of LS and AIC analysis allows us to give a slight preference for model II over model I, though the statistical analysis does not rule out model III.

As strike-slip earthquakes become width-limited at moments greater than $\sim 10^{20}$ Nm, the range of data available is narrower than for dip-slip earthquakes. Within the range $2 \times 10^{16} < M_0 < 5 \times 10^{19}$, the $M_0 \sim A$ data (Fig. 6) have a slope of 0.64 ($\gamma = 1.56$) and r of 0.95; the AIC results for the four models are −50, −57, −50, and −32, respectively. The $M_0 \sim L$ data (Fig. 7) have $\delta = 2.48$ and r of 0.93, with AIC values of 18, 11, 14, and 52 for the four displacement models. Displacement model II is clearly preferred by the AIC analysis and slightly preferred by the LS analysis, though the statistical analysis does not rule out models I and III.

For the SCR earthquakes using the $M_0 \sim A$ data, the least-squares analysis gives a slope of 0.67 ($\gamma = 1.50$) and r of 0.99, with the AIC for the four models being −21, −24, −20, −10, respectively. The $M_0 \sim L$ data have $\delta = 2.48$ and r of 0.97, with the AIC for the four models being 3.6, 5.2, 8.0, and 13.0, respectively. This gives equal weighting to models I and II.

Overall, model II ($\bar{D} \propto \sqrt{A}$) gives the best fit to the available data and is adopted here. Model I has a slightly poorer fit to the data, but, as it cannot be ruled out, empirical results for this model are also provided. Model III is worse fit to the data than either models I and II, and while statistically it cannot be excluded, I do not examine this model further. Model IV is a poor fit to all the data and I exclude it as a

Table 2
The Moment-Length and Moment-Area Relations for the Four Displacement Models*

Model	$\bar{D} =$	$M_0 \propto$	$\log M_0 \propto \delta =$	δ for $\beta = 2/3$	$\log M_0 \propto \gamma =$	γ for $\beta = 2/3$
1	$C_2 W$	$\mu L^{1+2\beta}$	$(1 + 2\beta) \log L$	2.33	$(1 + 2\beta)/(1 + \beta) \log A$	1.4
2	$C_2 \sqrt{A}$	$\mu L^{3/2(1+\beta)}$	$3/2(1 + \beta) \log L$	2.5	$3/2 \log A$	1.5
3	$C_2 L$	$\mu L^{2+\beta}$	$(2 + \beta) \log L$	2.67	$(2 + \beta)/(1 + \beta) \log A$	1.6
4	$C_2 L^{2-\beta}$	μL^3	$3 \log L$	3	$3/(1 + \beta) \log A$	1.8

*The expected values of γ and δ are compared with the least-squares estimate of slope from the $M_w \sim A$ or $M_w \sim L$ data, in order to determine a preferred displacement model. Note that by combining various β (e.g., 0.0, 0.667, 1.0) with the four displacement models, these equations describe almost all common fault-scaling models.

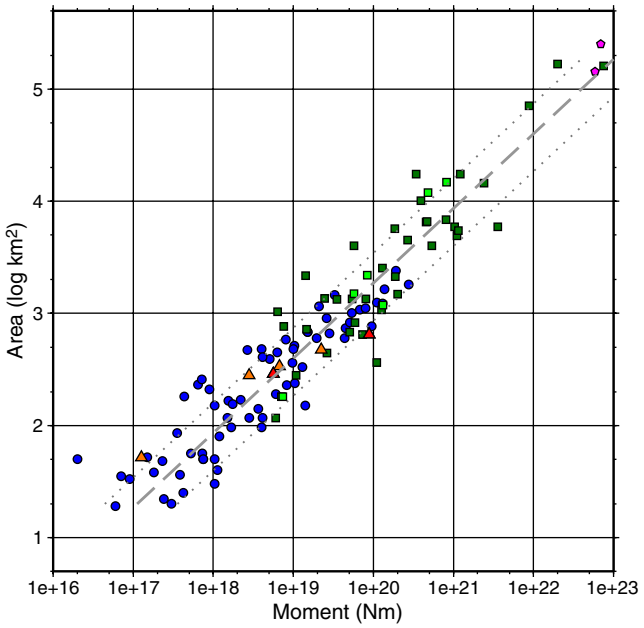

Figure 4. The M_0 versus area data for dip-slip earthquakes The gray dashed line is the constrained least squares (CLS), with a fixed slope of 2/3, best fit to the data and the gray dotted lines are $\pm 1\sigma$ uncertainties. The color version of this figure is available only in the electronic edition.

viable displacement model for all earthquake types. For $\beta = 2/3$ the displacement model is $D = C_2\sqrt{A} = C_2\sqrt{C_1 L^{5/6}}$. Substituting these relations into the definition of moment allows a series of M_0, $\bar{D}$, W, L, and A relations (equations 7–13) to be derived.

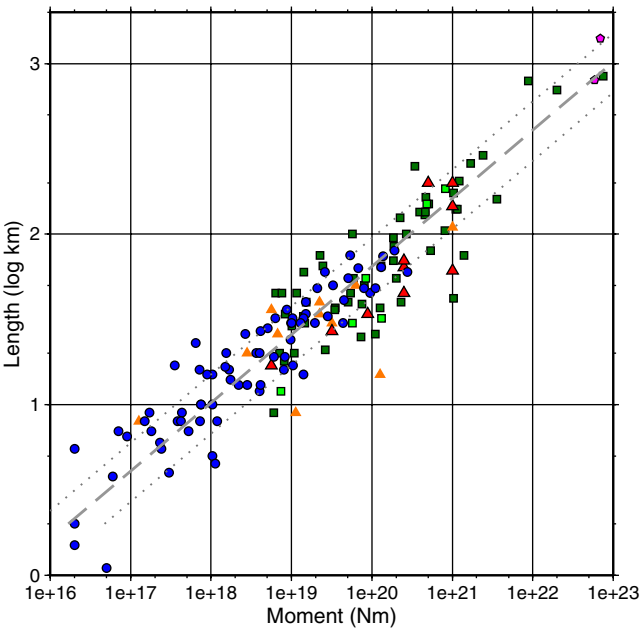

Figure 5. The M_0 versus length data for dip-slip earthquakes The gray dashed line is the CLS, fixed to a slope of 2/5, best fit to the data and gray dotted lines are $\pm\sigma$. The color version of this figure is available only in the electronic edition.

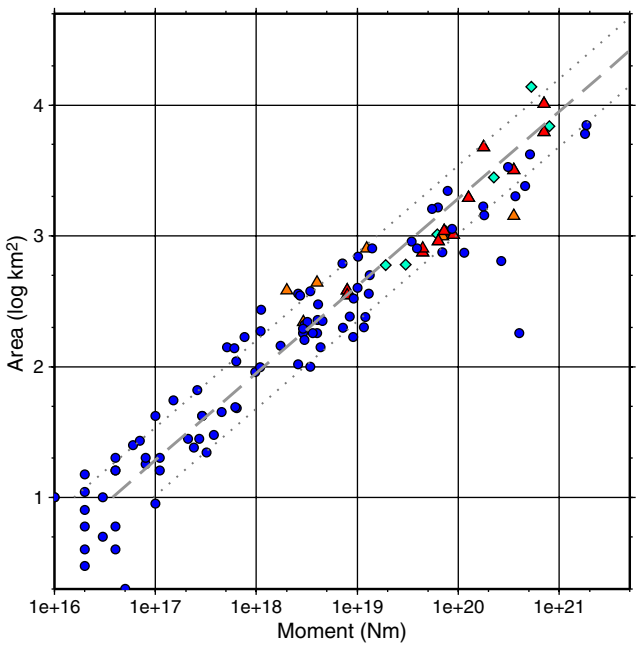

Figure 6. The M_0 versus area data for strike-slip interplate earthquakes. The gray dashed line is the CLS best-fit to the data for areas between 20 km^2 and 800 km^2. Above 800 km^2 the slope is assumed to be 2/3 for a $\sqrt{A}$ displacement model. The color version of this figure is available only in the electronic edition.

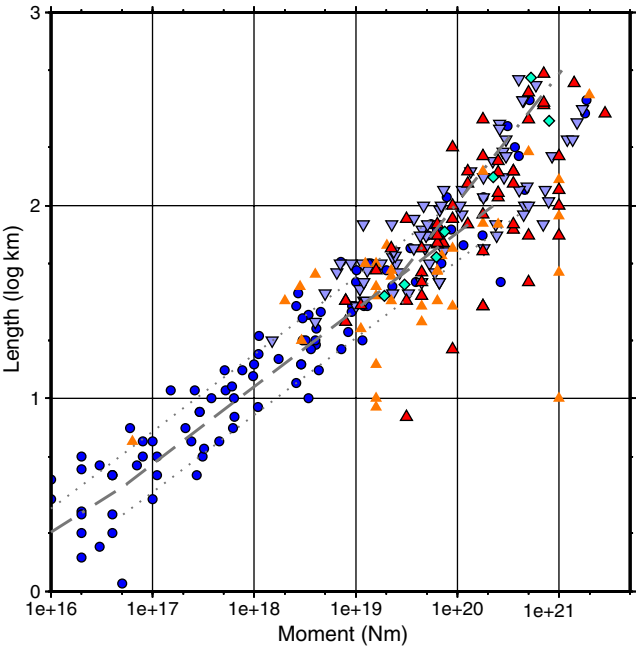

Figure 7. The M_0 versus length data for strike-slip earthquakes. Between 3.4 and 45 km, the gray dashed line is the CLS, fixed to a slope of 2/5, best fit to the data. Above 45 km the slope is assumed to be 1/1.5 (see discussion of strike-slip earthquakes in text) and below 3.4 km it is 1/3. Above 45 km the dashed lines follows the cluster Romanowicz and Ruff (2002) identified as A class, with the cluster at higher moments being their B class earthquakes. The color version of this figure is available only in the electronic edition.

$$W = C_1 L^{\beta} \quad \text{where} \quad \beta = 2/3 \tag{6}$$

$$\log M_0 = 3/2 \log A + \log C_2 \mu \tag{7}$$

$$\log M_0 = 5/2 \log L + 3/2 \log C_1 + \log C_2 \mu \tag{8}$$

$$\log M_0 = 15/4 \log W - 2/3 \log C_1 + \log C_2 \mu \tag{9}$$

$$\log M_0 = 21/5 \log \bar{D} + 3/5 \log C_1 - 4/5 \log C_2 + \log \mu \tag{10}$$

$$\log \bar{D} = 1/2 \log A + \log C_2 \tag{11}$$

$$\log \bar{D} = 5/6 \log L + 1/2 \log C_1 + \log C_2 \tag{12}$$

$$\log \bar{D} = 7/6 \log W - 2/3 \log C1 + \log C_2 \tag{13}$$

$$\Delta\sigma \approx 8 \times 10^{10} C_2 \quad \text{when} \quad W = L \tag{14}$$

These nine equations apply to all dip-slip faults with a length greater than 5 km, and all strike-slip earthquakes with lengths greater than 5 km and lengths less than 40 to 100 km. The special case of large strike-slip faults is discussed in a separate section. The eight equations in Table 2 can be used to calculate the expected relations for a wide range of earthquake types. For example, small earthquakes have $\beta = 1.0$ and displacement models I–III become identical. For width-limited strike-slip earthquakes, $\beta = 0.0$. Hanks and Bakun (2002) proposed displacement model III, with $\beta = 1.0$ for small earthquakes and $\beta = 0.0$ for large earthquakes. Romanowicz and Ruff (2002) considered model I the preferred displacement model and assumed the same values for β.

I compared the values derived in equations (7–13) with those from several empirical studies. This is summarized in Table 3. Wells and Coppersmith (1994), Pegler and Das (1996), and Henry and Das (2001) are all empirical analyses of fault dimensions estimated from aftershocks. Within the quoted errors, almost all the empirical results are consistent with my results, the exception being the WC94 $M \sim L$ results. Because WC94 included the large fault width-limited earthquakes, I would expect their slope to be smaller, and that is what is observed. The Mai and Beroza (2000) data are from finite-fault inversion techniques; their results are all consistent with my results, as are the Liu-Zeng, Heaton and DiCaprio (2005) results, which used a stochastic model to explore the effect of slip heterogeneity on slip-length scaling for strike-slip faults. Their $D \sim L$ values are the range of values for which their model matched the observed data. They also showed that only this range of values (0.75–1.0) are consistent with Gutenberg–Richter statistics with $b = 1.0$.

The slope of relations in equations (7–13) are a result of my identifying a power law relationship for the area of fault ruptures (equation 6), the empirical estimation of $\beta = 2/3$, the selection of a displacement model , and substituting these into the definition of seismic moment. That all the predicted slopes in equations (7–13) are consistent with a diverse range

Table 3
Comparison of My Scaling Factors (Assuming $W = C_1 L^{\beta}$, $\beta = 2/3$, and $\bar{D} = C_2\sqrt{A}$) with Published Empirical Results*

	This Paper		WC94†		H&D		P&D	M&B‡		
			All	SS	DS	SS	SS	DS	SS	LHD§
$M_0 \sim A$	3/2	1.5	–	–	–	–	–	1.33 (0.2)	1.75 (0.4)	–
$M_w \sim A$	–	1.0	0.98	1.02	–	–	–	–	–	–
$M_0 \sim L$	5/2	2.5	–	–	2.7 & 2.2	2.7	>2	2.5 (0.27)	2.5 (0.24)	–
$M_w \sim L$	–	1.67	1.49	1.49	–	–	–	–	–	–
$M_0 \sim L$	3/2	1.5	–	–	–	–	–	–	–	–
$M_0 \sim W$	15/4	3.75	–	–	–	–	–	2.9 (0.8)	5.9 (1.5)	–
$M_w \sim W$	–	2.25	2.25	2.59	–	–	–	–	–	–
$M_0 \sim D$	3	–	–	–	–	–	–	4.0 (1.5)	3.45 (0.6)	–
$M_w \sim D$	2	–	–	–	–	–	–	–	–	–
$D \sim L$‖	5/6	0.83	0.82	0.89	~1	~1	–	–	–	0.75–1.0
$D \sim W$	5/4	1.25	–	–	1.0–1.5	1.0–1.5	–	–	–	–

*The numbers in parentheses are the uncertainties reported.

†WC94 (Wells and Coppersmith, 1994), H&D (Henry and Das, 2001), and P&D (Pegler and Das, 1996) are all empirical analyses of fault dimensions estimated from analysis of aftershocks.

‡M&B (Mai and Beroza, 2000) data are from finite-fault inversion techniques.

§LHD (Liu-Zeng, Heaton, and DiCaprio, 2005) used a stochastic model to explore the effect of slip heterogeneity on slip-length scaling for strike-slip faults.

‖The $D \sim L$ numbers are the range of values for which their model matched the observed data. They also showed that only this range of values (0.75–1.0) is consistent with Gutenberg–Richter statistics with $b = 1.0$ results of the constrained least-squares analysis of the $M_0 \sim A$ and $M_0 \sim L$ data.

of published scaling relations is strong validation for my proposed area power law and the derived scaling relations.

Part 2: Empirical Scaling Relations

For a fixed β, equations (7–14) constitute a self-consistent model of earthquake fault scaling with the only two variables, C_1 and C_2. Here I estimate these variables from the empirical data for various types of earthquakes to develop type-specific scaling relations. The three types of earthquakes are plate boundary strike-slip, plate boundary dip-slip, and intraplate continental dip-slip earthquakes.

Method

Determining empirical fault-scaling relations usually involves an ordinary least-squares estimate of the form $\log M_0$ (or M_w) $= a + b \log$ (L or A), where a and b and their uncertainties are empirically derived. This was the approach of WC94 and Stirling *et al.* (2002). Here I follow the approach of Hanks and Bakun (2002) and Somerville *et al.* (1999): I constrain the slope b to the relevant value given in equations (6–8) and use the least-squares method to estimate a. I refer to this as constrained least squares. The constant C_1 is estimated using equation (6) from the length versus width data. The constant C_2 is estimated using equations (7) and (8) from the $M_0 \sim A$ and $M_0 \sim L$ data. The estimates of C_1 and C_2 are validated against the $\bar{D} \sim A$ and $\bar{D} \sim L$ data using equations (11) and (12).

Note that converting area and length from m to km requires the constants -9 $(1/\log 1000^{2*1.5})$ and -7.5 $(1/\log 1000^{2.5})$, respectively, to be added to the equations where $\log A$ (e.g., equation 7) and $\log L$ (e.g., equation 8) appear. The meter version of equation (6) requires the constant C_1 to be scaled by $1/10$ $(1/1000^{1/3})$.

Results

The empirical results for C_1 and C_2, along with their standard deviations, are summarized in Table 4. A value of $\mu = 3.3 \times 10^{10}$ Pa is used to calculate C_2 from $C_2\mu$, which is estimated from the $M_0 \sim A$ data. The same value is used, along with the preferred value of C_1, to calculate C_2 from $C_1^{3/2}C_2\mu$, which is estimated from the $M_0 \sim L$ data. The preferred values can be substituted into equations (6–14) to obtain many combinations of scaling relations. In the discussion that follows, readers are referred back to Figures 1–7.

For the dip-slip interplate earthquake data (Fig. 1), the best fit gives $C_1 = 17.5m^{1/3}$ with the upper and lower 1σ prediction intervals being $C_1 = 25.0$ and $C_1 = 12.5$, respectively. The $M_0 \sim A$ data (Fig. 4) give a value of $C_2 = 3.8(1.5–12) \times 10^{-5}$. The $M_0 \sim L$ data (Fig. 5), using $C_1 = 17.5$, give a value of $C_2 = 3.9(1.6–13) \times 10^{-5}$. The two estimates of C_2 differ by only 8%, which considering that they are derived from different data, as well as the uncertainties in estimating both C_1 and C_2, is a very small difference.

For strike-slip earthquakes, the range over which C_1 has been estimated is 4–35 km for the $L \sim W$ data (Fig. 2). This narrow range increases the uncertainty in estimating C_1. The best-fit regression gives $C_1 = 15m^{1/3}$, with the upper and lower bounds being $C_1 = 20.0$ and $11m^{1/3}$, respectively. The estimates for C_2 are 3.6×10^{-5} and 3.7×10^{-5} for the

Table 4
Empirically Estimated Constants Used in Equations (6–14) to Relate Moment with Fault Area, Length, and Displacement*

Data	C_1 ($m^{1/3}$)	$C_2 \times 10^{-5}$	$\Delta\sigma$ (MPa)	Area/Length Range† (km)
Interplate Dip-Slip				
$W \sim L$	17.5 (12–25)	–	–	5.5–1,400
$M_0 \sim A$	–	3.8 (1.5–12)	3.0	0–300,000
$M_0 \sim L$	–	3.9 (1.6–13)	3.1	5.5–1,400
$M_0 \sim A$ ‡	–	2.7	2.2	1,000–300,000
$M_0 \sim L$ ‡	–	3.3	2.6	50–1,400
Preferred	17.5 (12–25)	3.8 (1.5–12)	3.0	–
Interplate Strike-Slip				
$W \sim L$	15.0 (11–20)	–	–	3.4–50
$M_0 \sim A$	–	3.6 (1.5–9.1)	2.9	15–1,000
$M_0 \sim L$	–	3.7 (1.4–8.6)	3.0	3.4–50
Preferred	15.0 (11–20)	3.7 (1.5–9.0)	3.0	–
SCR Dip-Slip				
$W \sim L$	13.5 (11–17)	–	–	2.5–100
$M_0 \sim A$	–	7.3 (5.4–10)	5.8	0–500
$M_0 \sim L$	–	7.3 (3.1–15)	5.8	2.5–50
Preferred	13.5 (11–17)	7.3 (5.0–10)	5.8	–

*Note that $C_2\mu$ is empirically estimated and $\mu = 3.3 \times 10^{10}$ has been used to estimate C_2.
†The range is the range used in the constrained least-squares analysis.
‡These are the estimates when the small number of earthquakes with moment $> 20^{21}$ Nm are given more weight.

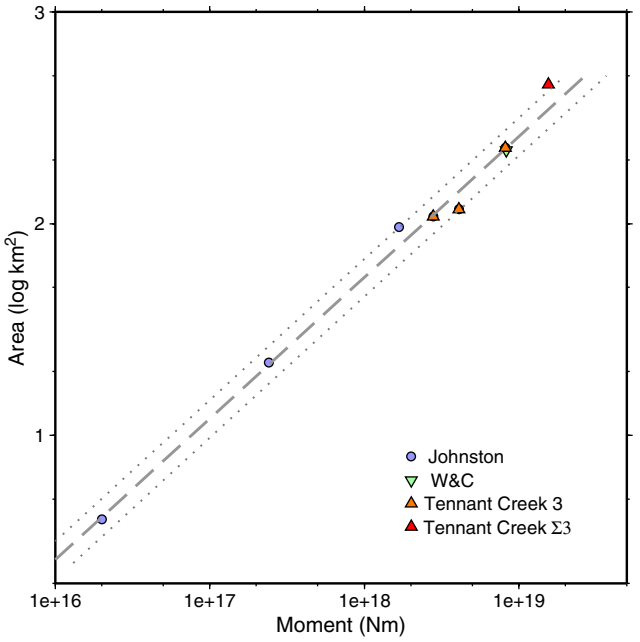

Figure 8. The M_0 versus area data for dip-slip SCR faults. The data have less scatter than the interplate data, possibly reflecting the relative uniformity of the SCR tectonic and geologic environments compared with the interplate environments. The color version of this figure is available only in the electronic edition.

$M_0 \sim A$ and $M_0 \sim L$ data, respectively (Figs. 6, 7). These estimates are almost identical to the values derived from the dip-slip data (Table 4).

For intraplate (SCR) scarp-forming earthquakes, the best fit to the $W \sim L$ data (Fig. 3) gives $C_1 = 13.5m^{1/3}$, with

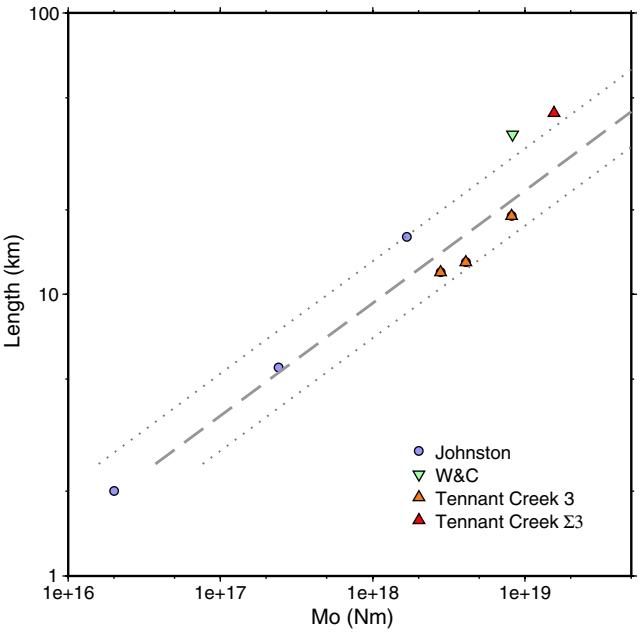

Figure 9. The M_0 versus length data for dip-slip SCR earthquakes. The data have relatively low scatter. The color version of this figure is available only in the electronic edition.

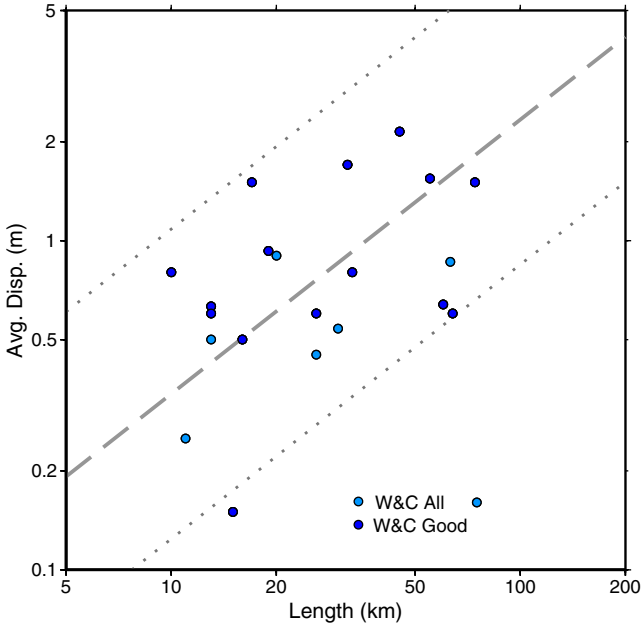

Figure 10. Dip-slip interplate average displacement versus length data. The dashed line is predicted from equation (12) using the values of C_1 and C_2 estimated from the $L \sim W$, $M_0 \sim A$, and $M_0 \sim L$ data. The dotted lines are the uncertainties estimated from the uncertainties in C_1 and C_2. The predicted displacements are an excellent fit to the actual displacements. The color version of this figure is available only in the electronic edition.

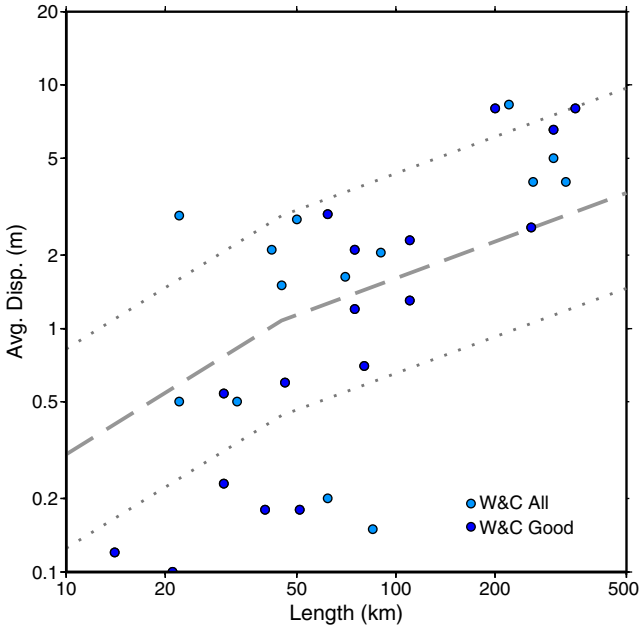

Figure 11. Strike-slip interplate average displacement versus length data. The dashed line is predicted from equation (12) using the values of C_1 and C_2 and the dotted lines are the uncertainties estimated form the uncertainties in C_1 and C_2. The slope above 45 km assumes $D \propto A^{1/2}$, with all the lines being extrapolations beyond 45 km. The predicted displacements are a good fit to the actual displacements. The color version of this figure is available only in the electronic edition.

the respective upper and lower estimates being $C_1 = 10.5$ and $20.0m^{1/3}$. The $M_0 \sim A$ data (Fig. 8) give a value of $C_2 = 7.3 \times 10^{-5}$, and the $M_0 \sim L$ data (Fig. 9) give $C_2 = 7.3 \times 10^{-5}$. Using equation 14 with $C_2 = 7.3(5–12) \times 10^{-5}$ gives a stress drop ($\Delta\sigma$) of 5.8(4.0–9.6)MPa. Of the 870 SCR earthquakes, Johnston (1994) identified 44 earthquakes where stress drop had been derived from either the seismic source function duration (τ) or corner frequency. Johnston concluded that the corner frequency method was not as robust, leaving 39 earthquakes for analysis. Using the same technique as Somerville *et al.* (1987), Johnston concluded that stress drop was constant with $\log M_0$, with a median value of 8.3 (2.5–25)MPa, which are consistent with my values.

As a test of the relations, I compare the predicted displacement with displacement data for the three classes of earthquake. For the dip-slip interplate average displacement versus length data (Fig. 10), the relation predicted by substituting C_1 and C_2 into equation (12) bisects the data and predicted uncertainties bracket the data. The predicted displacements are an excellent fit to the actual displacements. Similarly the strike-slip data are a very good fit to the predicted displacement models. The break in displacement when the faults become width constrained can be clearly seen in Figure 11. The SCR displacement data plot (Fig. 12) as two separate clusters with D_{max} being about twice D_{av}, which is consistent with the findings of WC94. The predicted displacement is within the scattered data and only about 25% higher than the center of both the $D_{av} \sim$ RLD and $D_{av} \sim$ SRL clusters. As the displacement data were not used in calculating the prediction equation and given the large uncertainties in measuring average slip, this is an excellent fit to the empirical data for all three classes of faults. The excellent fit to the displacement data gives us confidence in the proposed relations.

The previously discussed results have used subsurface rupture length (RLD), not surface rupture length (SRL), for L. Wells and Coppersmith (1994) estimated that on average the SRL was 0.75 of the RLD, with the 95% range being 0.3–1.1, though they noted that there is a length dependency (WC94, figure 2). The relation $\log \mathrm{SRL} = 1.1 \log \mathrm{RLD} - 0.275$ is a better least-squares fit to the data than the $\mathrm{SRL} = 0.75 \times \mathrm{RLD}$ of WC94. Substituting this into equation (8) and using the interplate dip-slip values gives $\log M_0 = 2.5 \log L + 7.96 = 2.27 \log \mathrm{SRL} + 8.59$ and $M_w = 1.67 \log L + 4.24 = 1.52 \log \mathrm{SRL} + 4.66$. For strike-slip earthquakes, the values of C_1 and C_2 give the relation $M_w = 1.67 \log L + 4.17 = 1.52 \log \mathrm{SRL} + 4.58$. Assuming SRL = RLD for SCR scarps is a better fit to the data than the interplate earthquakes relationship proposed previously.

Table 5 gives the various scaling relations for three classes of faults discussed. The values are obtained by substituting the relevant values of β, C_1, and C_2, and their respective uncertainties, into equations (6–13). The more

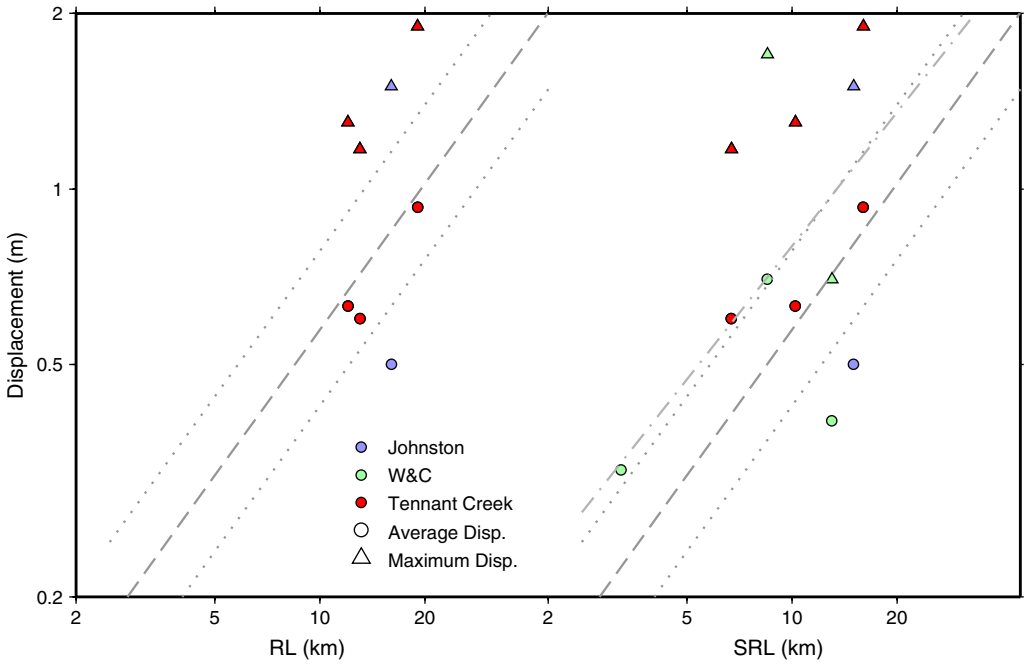

Figure 12. For dip-slip (SCR) earthquakes, the surface rupture length (SRL), and rupture length (RL) versus displacement data. The gray dashed line is the relation predicted from the estimates of C_1 (13.5) and C_2 (7.3×10^{-5}) with the dotted lines being the predicted range from the C_2 1σ values (12×10^{-5}, 5×10^{-5}). The predicted displacements are an excellent fit to the actual displacements. The line on the SRL plot incorporates the $\log(\mathrm{SRL}) = 1.1 \times \log(\mathrm{RLD}) - 0.275$ relation and is a worse fit to the displacement data than assuming SRL = RLD. The maximum displacement data are about double the average displacement data. The color version of this figure is available only in the electronic edition.

Table 5
Summary of Constants for the More Common Fault-Scaling Relations, in Meters and Newtons

		a*	b*	$S(b)^{\dagger}$	Range A (m^2), L (m)
DS					
	$\log(W) = a \times \log(L) + b$	0.667	1.24	1.15–1.40	$>5,500$
	$\log(D_{Av}) = a \times \log(A) + b$	0.5	−4.42	−4.82– − 3.92	>0
	$\log(D_{Av}) = a \times \log(L) + b$	0.833	−3.80	−4.21– − 3.29	$>5,500$
	$\log(M_0) = a \times \log(A) + b$	1.5	6.10	5.69–6.60	>0
	$\log(M_0) = a \times \log(L) + b$	3.0	6.10	–	0–5,500
		2.5	7.96	7.53–8.51	$>5,500$
	$\log(M_0) = a \times \log(\mathrm{SRL}) + b^{\ddagger}$	2.27	9.25	–	$>5,500$
SS					
	$\log(W) = a \times \log(L) + b$	0.667	1.18	1.04–1.30	3,400–45,000
	$\log(D_{Av}) = a \times \log(A) + b$	0.5	−4.43	−4.82– − 4.05	>0
	$\log(D_{Av}) = a \times \log(L) + b$	1.0	–	–	0–3,400
		0.833	−3.84	−4.24– − 3.45	3,400–45,000
		0.5	−2.29	−2.72– − 1.93	$>45,000$
	$\log(M_0) = a \times \log(A) + b$	1.5	6.09	5.69–6.47	>0
	$\log(M_0) = a \times \log(L) + b$	3.0	6.09§	5.65–6.52§	0–3,400
		2.5	7.85	7.41–8.28	3,400–45,000
		1.5	12.50§	12.01–12.88§	$>45,000$
	$\log(M_0) = a \times \log(\mathrm{SRL}) + b$	2.27	9.15	–	3,400–65,000
		1$^{\|}$	15.26$^{\|}$	–	$>65,000$
SCR					
	$\log(W) = a \times \log(L) + b$	0.667	1.13	1.04–1.23	$>2,500$
	$\log(D_{Av}) = a \times \log(A) + b$	0.5	−4.14	−4.30– − 4.00	>0
	$\log(D_{Av}) = a \times \log(L) + b$	0.833	−3.57	−3.72– − 3.43	$>2,500$
	$\log(M_0) = a \times \log(A) + b$	1.5	6.38	6.22–6.52	>0
	$\log(M_0) = a \times \log(L) + b$	3.0	6.39	–	0–2,500
		2.5	8.08	7.87–8.28	$>2,500$
	$\log(M_0) = a \times \log(\mathrm{SRL}) + b$	2.5$^{\#}$	8.08$^{\#}$	–	–

*The value of a and b in each row is the value applicable to the algebraic equation in the first column of that row.

$^{\dagger}S(b)$ are the uncertainties calculated from the uncertainties in C_1 and C_2 that were estimated from the $W \sim L$, $M_0 \sim A$, and $M_0 \sim L$ data.

‡SRL variables are derived by substituting the relation $\mathrm{SRL} = 1.1 \log \mathrm{RLD} - 0.275$ into the L results.

§These values were set so they intersect with the values estimated from the data between 3.4 and 40 km, where $a = 2.5$.

$^{\|}$These values are set such that they meet the previously identified relation at 65 km and the moment at 400 km is identical for both SRL and L relations.

$^{\#}$The data suggest that for SCR the relation SRL = RLD is preferred so the SLR and L relations are identical.

common M_w relations and $\bar{D} \sim L$ relations are summarized in Table 6. These are primarily given to allow ready comparison of my results to other well-known scaling relations, for example, WC94 and the Working Group on California Earthquake Probabilities (WGCEP, 2003, 2007). To avoid the complexities arising from mixing units (i.e., m and km) when applying my relations, I suggest practitioners use the M_0 and meter-based relations given in Table 5.

Discussion

As discussed previously, when deriving the $\log M_0 \propto 3/2 M_S$ relation, Kanamori and Anderson (1975) explicitly assumed that $M_0 \propto L^3$ and assumed three similarity conditions: (1) $L/W = \text{const}$ (constant aspect ratio); (2) $D/W = \text{const}$ (constant stress drop); and (3) $vt/L = \text{const}$ (dynamic similarity). When Kanamori (1977) and Hanks and Kanamori (1979) developed the moment magnitude scale (M_w $2/3 \log M_0 - 6.07$), they based this on these M_S and M_0 relations. As I have shown, $L/W = \text{const}$ does not hold above $M_0 \approx 10^{17}$ Nm ($M_w \approx 5.3$), in which case the relations $M_0 \propto L^3$ and $M_0 \propto A^{3/2}$ cannot both hold. The constant in the moment magnitude scale should perhaps be $1/\gamma$, which if $D \propto \sqrt{A}$ is $1/1.5$. If $D \propto W$ or $D \propto L$ apply, then for $\beta = 2/3$ the constant would be $1/1.4$ or $1/1.6$, respectively.

Table 6
The Most Commonly Used M_w, A, L, and D_{av} Relations

	a*	b*
$M_w = a \log A + b$ (in km^2)		
DS	1.0	4.00
SS	1.0	3.99
SCR	1.0	4.19
$M_w = a \log L + b$ (L in km)		
DS	1.67	4.24
SS	1.67	4.17
SCR	1.67	4.32
$M_w = a \log \mathrm{SRL} + b$ (L in km)		
DS†	1.52	4.40
SS	1.52	4.33
SCR‡	1.67	4.32
$\log(D_{av}) = a \log L + b$ (D_{av} in m, L in km)		
DS	0.833	−1.30
SS	0.833	−1.34
SCR	0.833	−1.07
Stress Drop MPa		
DS	3.04	–
SS	2.96	–
SCR	5.84	–

*The value of a and b in each row is the value applicable to the algebraic equation in the first column of that row.

†These SRL variables are derived by substituting the relation $\mathrm{SRL} = 1.1 \log \mathrm{RLD} - 0.275$ into the L results.

‡Because the earthquakes in SCR tend to be shallow (< 10 km), the SRL = RLD is assumed and this relation is not preferred in SCR. These have been included to allow simple comparison to other results (e.g., WC94), but my suggestion is that the M_0-based relations given in Table 5 be used in practice.

In the relation $W = C_1 L^{\beta}$, I chose $\beta = 2/3$ over the purely empirical value (e.g., 0.668) primarily to simplify the expected values of γ and δ. Proving or disproving that $\beta = 2/3$ is beyond the scope of this paper. To even demonstrate that $\beta \approx 2/3$ in all tectonic and geological environments via empirical analysis of fault-scaling data would require significantly improved datasets. To prove it will require vastly improved datasets. Other possibilities are the fields of numerical fault simulation and rupture modelling. I note that power laws with an exponent of $2/3$ are relatively common in nature; for example, the number of earthquakes versus M_0 (Scholz, 2002), animal size (White and Seymour, 2003), fire front intensity (Albini, 1981), and friction and normal forces (Riedo *et al.*, 2004). Such power law relationships are often indicators that a system is a self-organizing complex or self-similar system (Peitgen *et al.*, 1992). This suggests that while there appears to be a change in the physics governing the rupture process for faults of length more than 2–6 km (see the following discussion), the rupture process is still a self-similar system.

For interplate dip-slip, interplate strike-slip, and SCR earthquakes, $L = W$ when $L = 5.5$ (2–15) km, 3.4 (1.3–8.0) km, and 2.5 (1.1–5.0) km, respectively. Below these sizes, faults are presumed to act as cracks with L^3 (e.g., Brune model) scaling. These sizes suggest that, above magnitudes 5.6, 5.1, and 5.0 for dip-slip, strike-slip, and SCR earthquakes, respectively, earthquakes have $L^{2.5}$ scaling; below this, they have L^3 scaling. The size of the interplate areas (11–30 km^2) are consistent with the typical size of asperities (Somerville *et al.*, 1999), suggesting the possibility that small earthquakes can be approximated as circular cracks up until the size of the local asperities, above which they follow the power law. The smaller size at which SCR earthquakes begin to follow the power law might be due to stronger faults, resulting in smaller asperities.

One interpretation of the constant C_1 is that it depends on the dimension at which a rupture transitions from having a constant aspect ratio to following a power law. C_2 controls the amount of displacement for a given area and so stress drop. It is likely that these two constants vary between different tectonic environments, which would account for much of the scatter in the data. This is consistent with the results of Romanowicz and Ruff (2002) and Manighetti *et al.* (2007), discussed previously. Unfortunately, current datasets are not sufficiently comprehensive to meaningfully develop constants (C_1 and C_2) for specific tectonic regimes. For example, the data used by Romanowicz and Ruff (2002) do not contain any width or displacement information. This is common to much of the previous work discussed in this paper. The relative uniformity of the SCR tectonic environment could explain the very small scatter in the SCR $M_0 \sim A$ and $M_0 \sim L$ data, suggesting that with improved datasets, region- or tectonic-specific relations might be possible.

Division of the data into regional and/or tectonic division might dramatically reduce the uncertainty within each division. If this were the case, this would reduce the epistemic uncertainty for each region. Aleatory uncertainty will always remain, but if the overall uncertainty can be reduced by reducing the epistemic uncertainty, it would greatly improve the usefulness of scaling relations. For example, the range of C_2 for SCR, strike-slip, and dip-slip faults is 2, 6, and 9, respectively. A reduction of the uncertainty of continental strike-slip faults to that of SCR faults would significantly improve the quality of ground-motion prediction for this class of earthquakes.

In a probabilistic earthquake or tsunami hazard assessment, it is normal to sample the uncertainty space. One option would be to sample the uncertainty in the displacement model and so also use $\gamma = 1.4$ and $\gamma = 1.6$, for which C_2 is respectively 2.5×10^{-5} and 5.4×10^{-5} for strike-slip and 3.0×10^{-5} and 4.8×10^{-5} for dip-slip earthquakes. This could be implemented via a simple logic tree. While a valid approach, this is not my preferred option; I would prefer to only use $\gamma = 1.5$ and to more thoroughly sample the uncertainties in C_2 given in Table 5. Table 5 gives the basic M_0 relations that would be used for such assessments. As the results are sensitive to the range of C_2 and relatively insensitive to $1.4 \le \gamma \le 1.6$, for a fixed number of simulations

thoroughly sampling C_2 for $\gamma = 1.5$ would be more robust than also sampling γ at the expense of sampling C_2.

What stress drop is, how it is calculated, its physical meaning, and its applicability to earthquake hazard studies are widely debated topics (e.g., Atkinson and Beresnev, 1997). Various authors suggest stress drop increases, decreases, or remains constant with earthquake size (e.g., Abercrombie and Leary, 1993; Ide and Beroza, 2001). In the stress drop equation L_C, a characteristic length is considered the smallest dimension in the rupture plane (Aki, 1966; Bodin and Brune, 1996; Mai and Beroza, 2000). Assuming $L_C = W$, the scaling relations proposed in this paper imply $\Delta\sigma \propto L^{1/6}$ and $\Delta\sigma \propto M_0^{1/15}$, or taking into account the results of Sato (1972), $\Delta\sigma \propto L^{1/9}$ for dip-slip and $\Delta\sigma \propto L^{1/18}$ for strike-slip earthquakes. Relative to the large uncertainties in calculating stress drop, the natural scatter in the data (Abercrombie and Leary, 1993), and considering the ranges for which my proposed relations apply (e.g., 5–1500 km and 5–60 km), these changes in stress are very small. Therefore, an assumption of constant stress drop could not be disproved.

As fault rupture inversions become more accurate and consistently calculated and are calculated for past earthquakes, the resulting datasets might enable the vexing questions on stress drop to be resolved. This data, along with traditional data, when combined with tectonic and geological information (e.g., regional strain rates, crustal type, thickness, and age), might lead to a significant improvement in scaling relations. As mentioned previously, in the context of my model, I expect much of the uncertainty observed in C_1 and C_2 (i.e., epistemic uncertainty) might be accounted for by environment specific values.

Implications for Scaling of Large Strike-Slip Earthquakes

The relations I have proposed were developed primarily from dip-slip data. They also fit non-width-limited strike-slip earthquakes at least as well as previously published scaling models (e.g., WC94). So in the absence of evidence to the contrary, I assume they also apply to strike-slip earthquakes, out to fault lengths of 45 and possibly 100 km. Above this, large strike-slip earthquakes become fault width-limited ($\beta = 0$). If I assume that the $\bar{D} \propto \sqrt{A}$ displacement relation also applies to these large earthquakes, the resulting $M_0 \sim L$ model (Table 7) has three regimes: (1) $L < 3.4$ km $M_0 \propto L^3$, (2) $3.4 < L < 40$ km $M_0 \propto L^{2.5}$, and (3) $L > 40$ km $M_0 \propto L^{1.5}$, with $M_0 \propto A^{1.5}$ at all scales. I do not rule out other scaling models (e.g., $\bar{D} \propto W$), but as these scaling models have been very widely discussed in the literature, I do not propose to discuss them further. I consider that the empirical data lack sufficient precision to clearly prove or disprove any of these displacement models.

The resulting scaling relation for large strike-slip faults, $\log M_0 \propto 3/2 \log L$, is intermediate between W (or L^1) and L (or L^2) scaling. Several authors (Bodin and Brune, 1996; Mai and Beroza, 2000; Jung *et al.*, 2005; King and Wesnousky, 2007) have concluded that displacement is between the W and L scaling models. My model for strike-slip faults is similar to the continental, or class A, relation proposed by Romanowicz and Ruff (2002), but with $L^{1.5}$ instead of L^1 scaling applying at lengths greater than 50 km. The $L^{1.5}$ model has a similar fit to the width-limited $M_0 \sim L$ data that they interpreted as $L1$ scaling (Fig. 7). The other cluster, at $M_0 > 5 \times 10^{20}$ Nm in Figure 7, is Romanowicz and Ruff's (2002) oceanic class, which they interpreted as having a break in scaling at 100 km instead of 45 km.

Both Bodin and Brune (1996) and Shaw and Scholz (2001) proposed a constant stress drop, two-regime D–L model that is intermediate between W and L scaling. Using this model, Shaw (2009) developed a three-regime fault-scaling relation for strike-slip faults, with a crossover regime between 16 and 100 km. If I used a cutoff of 100 km instead of 50 km, and $\bar{D} \propto W$ instead of $\bar{D} \propto \sqrt{A}$ above the cutoff, my displacement model would be very similar to theirs. Like Hanks and Bakun (2002, 2008), Shaw (2009) explicitly assumes that faults scale with a constant aspect ratio of ~1 until they reach the width of the seismogenic zone (~16 km) and then become fixed width. I suggest that the empirical data (e.g., Fig. 2) do not support this assumption. However, as Shaw (2009) uses an intermediate displacement model for the crossover regime earthquakes, their model is likely insensitive to this assumption.

My $M_w \sim A$ relation is essentially identical to that of Wells and Coppersmith (1994) and Somerville *et al.* (2006), but gives smaller M than the linear models adopted by the Working Group on California Earthquake Probabilities (WGCEP, 2003, 2007; Ellsworth, 2003). For large earthquakes, the bilinear models proposed by Hanks and Bakun (2002, 2008) also estimate significantly more moment, and so displacement and static stress drop, for a given area. This

Table 7
Average Displacement, Width, Length, and Moment Relations for Strike-Slip Earthquakes, Assuming $\bar{D} = C_2\sqrt{A}$ Applies at All Scales

β =*	C_{1X}	C_{1X} units	$\bar{D}$ =	W =	M_0 =	km
1	1	–	$C_2\sqrt{C_{11}}L$	$C_{11}L$	$\mu C_{11}^{3/2} C_2 L^3$	0–5
2/3	15	$m^{1/3}$	$C_2\sqrt{C_1}L^{5/6}$	$C_1 L^{2/3}$	$\mu C_1^{3/2} C_2 L^{5/2}$	5–45
0	19000	m	$C_2\sqrt{C_{10}}L^{1/2}$	C_{10}	$\mu C_{10}^{3/2} C_2 L^{3/2}$	>45

*Note that $\log M_0 \propto 3/2 \log A$ for all β.

has significant implications for the recurrence of large earthquakes and on the expected ground motions simulated using such models.

Most authors tend to base their models primarily on $M_w \sim A$ or $M_w \sim L$ or $M_w \sim \bar{D}$ data only, with their models tending to be either $M_w \sim A$ or $M_w \sim L$ models only (e.g., Shaw and Scholz, 2001; Romanowicz and Ruff, 2002; Hanks and Bakun, 2002; Shaw, 2009), and with these models not generally being compared with each other. Authors who analyzed multiple data types (e.g., Wells and Coppersmith, 1994; Henry and Das, 2001; Mai and Beroza, 2000) have developed purely empirical relations and have not developed models that reconcile the scaling relations. This lack of comparison and reconciliation between various models and datasets limits the ability to quantitatively assess the models (e.g., relative weightings in a logic tree). As discussed previously, several authors have demonstrated that fault-scaling relations vary with tectonics, between geological regions, and with different methods for estimating rupture dimensions. I consider that more research that reconciles or at least isolates these three variables is needed before significant progress can be made in understanding the behavior of these very important (WGCEP, 2003, 2007) continental strike-slip earthquakes. Data from dip-slip faults are likely to contribute to constraining the relationships between geology, tectonics, and the scaling relations.

Conclusion

Seismic hazard and seismic risk assessments increasingly rely on assessment of multiple parameters (e.g., magnitude, rate of occurrence, extent of rupture), which ideally should be based on self-consistent relations among rupture area, rupture length, rupture width, and average displacement that apply across the magnitude/parameter ranges of interest for predictive equations. Specifically, the assumptions used to develop the M_w scale were a constant aspect ratio ($\beta = 1$) fault, $M_0 \propto L^3$, and $M_0 \propto A^{3/2}$. Because the aspect ratio is not constant, $M_0 \propto L^3$ and $M_0 \propto A^{3/2}$ cannot both be correct. I propose that the displacement relation $\bar{D} \propto \sqrt{A}$ applies to all faults and propose the fault area scaling relation $W = C_1 L^{\beta}$ where $\beta = 2/3$. By substituting $W = C_1 L^{\beta}$, $\beta = 2/3$, and $\bar{D} = C_2\sqrt{A}$ into the definition of moment ($M_0 = \mu \bar{D} L W$), I have developed a series of self-consistent scaling relations, relating seismic moment, fault rupture area, length, and displacement to each other. Above magnitude 5.6, 5.1, and 5.0 for dip-slip, strike-slip, and SCR earthquakes, respectively, earthquakes have $L^{2.5}$ scaling; below this, they have L^3 scaling. The relation $M_0 \propto A^{3/2}$, and so $M_w \propto 2/3 \log M_0$ applies at all scales. For very large ($M > 7.0$–7.6) strike-slip earthquakes, the applicability of $\bar{D} \propto \sqrt{A}$, and hence as $L^{1.5}$ scaling, as opposed to $\bar{D} \propto W$ or $\bar{D} \propto L$, and hence $L^{1.0}$ or $L^{2.0}$ scaling, remains ambiguous.

The slope of the linear log–log relations is dependent only on β, and $\beta = 2/3$ has been used to fix the slope in the constrained least-squares analysis of the available earthquake seismic moment, rupture area, length, width, and displacement datasets. This results in more robust scaling relations. When uncertainties and improved datasets are considered, the results are consistent with the fault-scaling relations of Wells and Coppersmith (1994). Unlike previous relations, these new relations are self-consistent. They enable fault moment, length, width, area, and displacement to be estimated from each other, with these estimates being consistent with the definition of seismic moment.

For fixed β, these relations have only two variables, C_1 and C_2. C_1 depends on the size at which a rupture transitions from having a constant aspect ratio to following the power law. C_2 controls the amount of displacement for a given area and so the static stress drop. It is likely that C_1 and C_2 vary between different tectonic and geological environments; most of the scatter in the empirical data might be explained by the mixing of data from different tectonic environments, rather than any inherent variability within a tectonic environment.

Data and Resources

All data used in this paper came from published sources listed in the references. Plots were made using the Generic Mapping Tools (Wessel and Smith, 1998).

Acknowledgments

I would like to thank G. Atkinson and P. Somerville for their suggestion that a reanalysis of the empirical data might be worthwhile. Discussions of the early results with J. Schneider were useful. Suggestions from the anonymous reviewers improved the manuscript.

References

Abe, K. (1975). Reliable estimation of the seismic moment of large earthquakes, *J. Phys. Earth* **23,** 381–390.

Abercrombie, R., and P. Leary (1993). Source parameters of small earthquakes recorded at 2.5 km depth, Cajon Pass, Southern California: Implications for earthquake scaling, *Geophys. Res. Lett.* **20,** no. 14, 1511–1514.

Akaike, H. (1974). A new look at the statistical model identification, *IEEE Trans. Auto. Contr.*, AC19, 716–723.

Aki, K. (1966). Generation and Propagation of G Waves from the Niigata Earthquake of June 16, 1964: Part 1. A statistical analysis, *Bull. Earthquake Res. Inst.* **44,** 23–72.

Aki, K. (1972). Earthquake Mechanism, in A. R. Ritdema (Editor), *The Upper Mantle, Tectonophysics* **13,** no. 1–4, 423–446.

Albini, F. A. (1981). A model for the wind-blown flame from a line of fire, *Combust. Flame* **43,** 155–174.

Atkinson, G., and I. Beresnev (1997). Do not call it stress drop, *Seism. Res. Lett.* **68**.

Atkinson, G., and D. Boore (2006). Ground motion prediction equations for earthquakes in eastern North America, *Bull. Seismol. Soc. Am.* **96,** 2181–2205.

Bodin, P., and J. N. Brune (1996). On the scaling of slip with rupture length for shallow strike-slip earthquakes: Quasistatic models and dynamic rupture propagation, *Bull. Seismol. Soc. Am.* **86,** 1292.

Boore, D. (1983). Stochastic simulation of high-frequency ground motions based on seismological models of the radiated spectra, *Bull. Seismol. Soc. Am.* **73,** 1865–1894.

Brune, J. N. (1970). Tectonic stress and the spectra of seismic shear waves from earthquakes, *J. Geophys. Res.* **75,** 4997–5009.

Brune, J. N. (1971). Correction, *J. Geophys. Res.* **76,** 5002.

Chinnery, M. A. (1969). Earthquake magnitude and source parameters, *Bull. Seismol. Soc. Am.* **59,** no. 5, 1969–1982.

Chlieh, M., J. Avouac, V. Hjorleifsdottir, T. A. Song, C. Ji, K. Sieh, A. Sladen, H. Hebert, L. Prawirodirdjo, Y. Bock, and J. Galetzka (2007). Coseismic slip and afterslip of the great M_w 9.15 Sumatra–Andaman earthquake of 2004, *Bull. Seismol. Soc. Am.* **97,** S152–S173.

Ellsworth, W. (2003). Appendix D—Magnitude and area data for strike slip earthquakes, in Working Group on California Earthquake Probabilities, Earthquake probabilities in the San Francisco Bay region—2002–2031, *U.S. Geol. Survey Open-File Rept. 03–214*, 6 p.

Engdahl, E. R., A. Villaseñor, H. R. DeShon, and C. H. Thurber (2007). Teleseismic relocation and assessment of seismicity (1918–2005) in the region of the 2004 M_w 9.0 Sumatra–Andaman and 2005 M_w 8.6 Nias Island great earthquakes, *Bull. Seismol. Soc. Am.* **97,** S43–s61.

Fujii, Y., and K. Satake (2007). Tsunami source of the 2004 Sumatra–Andaman earthquake inferred from tide gauge and satellite data, *Bull. Seismol. Soc. Am.* **97,** S192–S207.

Geller, R. J. (1976). Scaling relations for earthquake source parameters and magnitudes, *Bull. Seismol. Soc. Am.* **66,** no. 5, 1501–1523.

Hanks, T. C. (1977). Earthquake stress drops, ambient tectonic stress and stresses that drive plate motions, *Pure Appl. Geophys.* **115,** 441–458.

Hanks, T. C., and W. H. Bakun (2002). A bilinear source-scaling model for $M - \log A$ observations of continental earthquakes, *Bull. Seismol. Soc. Am.* **92,** no. 5, 1841–1846.

Hanks, T. C., and W. H. Bakun (2008). $M - \log A$ Observations for recent large earthquakes, *Bull. Seismol. Soc. Am.* **98,** no. 1, 490–494.

Hanks, T. C., and H. Kanamori (1979). A moment magnitude scale, *J. Geophys. Res.* **84,** no. B5, 2348–2350.

Henry, C., and S. Das (2001). Aftershock zones of large shallow earthquakes: Fault dimensions, aftershock area expansion and scaling relations, *Geophys. J. Int.* **147,** 272–293.

Ide, S., and G. Beroza (2001). Does apparent stress vary with earthquake size? *Geophys. Res. Lett.* **28,** no. 17, 3349–3352.

Johnston, A. C. (1994). Seismotectonic interpretations and conclusions from the stable continental region seismicity database, in *The Earthquake of Stable Continental Regions. Volume 1: Assessment of Large Earthquake Potential*,A. C. Johnston, K. J. Coppersmith, L. R. Kanter, and C. A. Cornell (Editors), Electric Power Research Institute.

Kanamori, H. (1977). The energy release in great earthquakes, *J. Geophys. Res.* **82,** no. 20, 2981–2987.

Kanamori, H., and D. L. Anderson (1975). Theoretical basis of some empirical relations in seismology, *Bull. Seismol. Soc. Am* **65,** no. 5, 1073–1095.

King, G. C. P., and S. G. Wesnousky (2007). Scaling of fault parameters for continental strike-slip earthquakes, *Bull. Seismol. Soc. Am.* **97,** no. 6, 1833–1840.

Liu-Zeng, J., T. Heaton, and C. DiCaprio (2005). The effect of slip variability on earthquake slip-length scaling, *Geophys. J. Int.* **162,** 841–849.

Madariaga, R. (1978). The dynamic field of Haskell's rectangular dislocation fault model, *Bull. Seismol. Soc. Am.* **68,** 869–887.

Mai, P. M., and G. Beroza (2000). Source scaling properties from finite-fault rupture models, *Bull. Seismol. Soc. Am.* **90,** 604–615.

Manighetti, I., M. Campillo, S. Bouley, and F. Cotton (2007). Earthquake scaling, fault segmentation, and structural maturity, *Earth Planet. Sci. Lett.* **253,** no. 3–4, 429–438.

Pegler, G., and S. Das (1996). Analysis of the relationship between seismic moment and fault length for large ctrustal strike-slip earthquakes between 1977–1992, *Geophys. Res. Lett.* **23,** 905–908.

Peitgen, H., H. Jurgens, and D. Saupe (1992). *Chaos and Fractals: New Frontiers of Science*, Springer-Verlang.

Rhie, J., D. Dreger, R. Bürgmann, and B. Romanowicz (2007). Slip of the 2004 Sumatra–Andaman earthquake from joint inversion of long-period global seismic waveforms and GPS static offsets, *Bull. Seismol. Soc. Am.* **97,** S115–S127.

Riedo, E., I. Palaci, C. Boragno, and H. Brune (2004). The 2/3 Power law dependence of capillary force on normal load in nanoscopic friction, *J. Phys. Chem.* **108,** no. 17, 5324–5328.

Romanowicz, B. (1992). Strike-slip earthquakes on quasi-vertical transcurrent faults: Inferences for general scaling relations, *Geophys. Res. Lett.* **19,** 481–484.

Romanowicz, B. (1994). Comment on "A Reappraisal of Large Earthquake Scaling" by C. Scholz, *Bull. Seismol. Soc. Am.* **84,** 1675–1676.

Romanowicz, B., and L. J. Ruff (2002). On moment-length scaling of large strike slip earthquakes and the strength of faults, *Geophys. Res. Lett.* **29,** 12.

Romanowicz, B., and J. B. Rundle (1993). On scaling relations for large earthquakes, *Bull. Seismol. Soc. Am.* **83,** no. 4, 1294–1297.

Sato, R. (1972). Stress drop for a finite fault, *J. Phys. Earth* **20,** 397–407.

Scholz, C. (1982). Scaling laws for large earthquakes: Consequences for physical models, *Bull. Seismol. Soc. Am.* **72,** no. 1, 1–146.

Scholz, C. H. (1994a). A reappraisal of large earthquake scaling, *Bull. Seismol. Soc. Am.* **84,** 215–218.

Scholz, C. H. (1994b). Reply to comments on "A reappraisal of large earthquake scaling", *Bull. Seismol. Soc. Am.* **84,** no. 5, 1677–1678.

Scholz, C. H. (1997). Size distributions for large and small earthquakes, *Bull. Seismol. Soc. Am.* **87,** no. 4, 1074–1077.

Scholz, C. H. (1998). A further note on earthquake size distributions, *Bull. Seismol. Soc. Am.* **88,** no. 5, 1325–1326.

Scholz, C. H. (2002). *The Mechanics of Earthquakes and Faulting*, Second Ed., Cambridge University Press, New York.

Scholz, C. H., C. A. Aviles, and S. G. Wesnousky (1986). Scaling differences between large interplate and intraplate earthquakes, *Bull. Seismol. Soc. Am.* **76,** no. 1, 65–70.

Shaw, B. E. (2009). Constant stress drop from small to great earthquakes in magnitude-area scaling, *Bull. Seismol. Soc. Am.* **99,** no. 2A, 871–875.

Shaw, B. E., and C. H. Scholz (2001). Slip-length scaling in large earthquakes: Observations and theory and implications for earthquake physics, *Geophys. Res. Lett.* **28,** no. 15, 2995–2998.

Shaw, B. E., and S. G. Wesnousky (2008). Slip-length scaling in large earthquakes: The role of deep-penetrating slip below the seismogenic layer, *Bull. Seismol. Soc. Am.* **98,** no. 4, 1633–1641.

Somerville, P. G., N. Collins, N. Abrahamson, R. Graves, and C. Saikia (2001). Earthquake source scaling and ground motion attenuation relations for the central and eastern United States, *Final Report to the U.S. Geological Survey, Contract No. 99HQGR0098*.

Somerville, P., N. Collins, and R. Graves (2006). Magnitude–rupture area scaling of large strike-slip earthquakes, *Final Report to U.S. Geological Survey, Grant No. 05HQGR0004*.

Somerville, P., K. Irikura, R. Graves, S. Sawada, D. Wald, N. Abrahamson, Y. Iwasaki, T. Kagawa, N. Smith, and A. Kowada (1999). Characterizing crustal earthquake slip models for the prediction of strong ground motion, *Seism. Res. Lett.* **70,** 59–80.

Somerville, P. G., J. P. McLarern, L. V. LeFevre, R. W. Burger, and D. V. Helmberger (1987). Comparison of source scaling relations of eastern and western North American earthquakes, *Bull. Seismol. Soc. Am.* **77,** no. 2, 322–343.

Stirling, M., D. Rhoades, and K. Berryman (2002). Comparison of earthquake scaling relations derived from data of the instrumental and preinstrumental era, *Bull. Seismol. Soc. Am.* **92,** no. 2, 812–830.

Thatcher, W., and T. C. Hanks (1973). Source parameters of southern California earthquakes, *J. Geophys. Res.* **78,** 8547–8576.

Vallée, M. (2007). Rupture properties of the giant Sumatra earthquake imaged by empirical Green's function analysis, *Bull. Seismol. Soc. Am.* **97,** S103–S114.

Wells, D. L., and K. J. Coppersmith (1994). New empirical relationships among magnitude, rupture length, rupture width, rupture area, and surface displacement, *Bull. Seismol. Soc. Am.* **84,** no. 4, 974–1002.

Wessel, P., and W. H. F. Smith (1998). New, improved version of the Generic Mapping Tools Released, *Eos Trans. AGU* **79,** 579.

White, C. R., and R. S. Seymour (2003). Mammalian basal metabolic rate is proportional to body mass 2/3, *Proc. Natl. Acad. Sci. USA* **100,** 4046–4049.

Working Group on California Earthquake Probabilities (WGCEP) (2003). Earthquake probabilities in the San Francisco Bay region: 2002 to 2031, *U.S. Geol. Surv. Open-File Rept. 2003-214*.

Working Group on California Earthquake Probabilities (WGCEP) (2007). The uniform California earthquake rupture forecast, version 2, *U.S. Geol. Surv. Open-File Rept. 2007-1437*.

Geoscience Australia
P.O. Box 378, Canberra
ACT, 2001, Australia
Mark.leonard@ga.gov.au

Manuscript received 23 July 2009